

# BiMind: A Dual-Head Reasoning Model with Attention-Geometry Adapter for Incorrect Information Detection

Anonymous ACL submission

## Abstract

Incorrect information poses significant challenges by disrupting content veracity and integrity, yet most detection approaches struggle to jointly balance textual content verification with external knowledge modification under collapsed attention geometries. To address this issue, we propose a dual-head reasoning framework, **BiMind**, which disentangles *content-internal reasoning* from *knowledge-augmented reasoning*. In BiMind, we introduce three core innovations: (i) an **attention geometry adapter** that reshapes attention logits via token-conditioned offsets and mitigates attention collapse; (ii) a **self-retrieval knowledge mechanism**, which constructs an in-domain semantic memory through kNN retrieval and injects retrieved neighbors via feature-wise linear modulation; (iii) the **uncertainty-aware fusion strategies**, including entropy-gated fusion and a trainable agreement head, stabilized by a symmetric Kullback-Leibler agreement regularizer. To quantify the knowledge contributions, we define a novel metric, **Value-of-eXperience (VoX)**, to measure instance-wise logit gains from knowledge-augmented reasoning. Experiment results on public datasets demonstrate that our BiMind model outperforms advanced detection approaches and provides interpretable diagnostics on when and why knowledge matters.

## 1 Introduction

Nowadays, with the rapid rise of social media platforms, such as X (Twitter), Instagram, and TikTok, an increasing number of individuals or communities rely on these online platforms for communication, information dissemination, and education, especially during the pandemic (Tsao et al., 2021). Though the conveniences brought by social media, the content correctness (i.e., factual accuracy and alignment with verifiable evidence) of information disseminated still falls short of media standards and

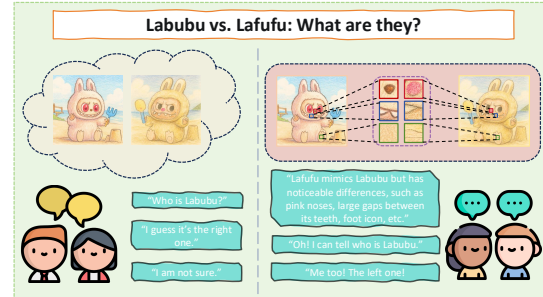


Figure 1: Illustrative case of self-correction via knowledge: without knowledge (left), the content-internal head labels Lafufu (counterfeit Labubu) as Labubu; with knowledge (right), the knowledge-augmented head corrects the label as Lafufu.

social expectations, compared to traditional media platforms, e.g., television and newspapers (Shu et al., 2017; Zhou and Zafarani, 2020). A large volume of unverified or distorted content is easily produced and propagated through social media platforms (Ahmed et al., 2022). Given that such incorrect information (e.g., spam (Wang et al., 2016), rumor (Bian et al., 2020a), etc.) has significant negative impacts on individuals and society, such as social trust and information credibility (Thorson et al., 2010; Bhattarai et al., 2021; Mazzeo et al., 2021), addressing incorrect information propagation has become crucial in the areas of social media, mass communication, and public health. Technically, automatic models are developed to identify and detect the incorrect information on social media platforms, thereby mitigating the social effects (Guo et al., 2020; Yang et al., 2023; Shi et al., 2023).

While incorrect information detection methods have achieved significant advancements, these methods still struggle with feature complexity, knowledge injection, and attention collapse. Specifically, prior work focuses either on textual content features (e.g., linguistic features and contextual embeddings) or on external knowledge (knowl-

edge graphs and retrieval-augmented generation), which integrates all the feature streams into a classifier, without any disentanglement between what is learned from textual content and what is contributed by external knowledge. As illustrated in Figure 1, without knowledge inputs, the reader potentially accepts the incorrect information (i.e., Lafufu) as correct (i.e., Labubu) from the raw content; once the reader obtains relevant knowledge, the information is corrected as incorrect.

To uncover the interplay between content reasoning and knowledge reasoning, we propose a new view: disentangling content reasoning from knowledge reasoning in an explicit and structured way. In this paper, we introduce a novel dual-head model architecture, **BiMind**, for incorrect information detection. Our model employs two separate heads to explore content and knowledge features, respectively, where the knowledge is retrieved from an in-domain memory. This separation mechanism allows us to measure, analyze, and apply the two streams of features in a structured way. Technically, our three contributions drive BiMind’s novelty:

- First, we introduce an attention geometry adapter (AGA) that reshapes attention distributions at the pre-softmax logit level, stabilizing text encoding by preventing attention collapse.
- Second, we design a self-retrieval knowledge module that encodes the training set into an in-domain semantic memory and then injects nearest-neighbor features via feature-wise linear modulation (FiLM).
- Third, we propose two uncertainty-aware fusion strategies, i.e., entropy-gated fusion and a trainable agreement head, where we adapt a symmetric Kullback–Leibler (KL) regularizer to ensure consistency between heads.
- Finally, we define a novel metric, Value-of-eXperience (VoX), to quantify the contributions from external knowledge, improving model interpretability.

Experimental results on four standard incorrect information datasets demonstrate that our model enhances detection accuracy and interpretability, especially when external knowledge contributes to model predictions.

## 2 Related Work

### 2.1 Content-based methods

Today, machine learning (ML) and natural language processing methods (Kadhim, 2019; Su et al., 2020) have emerged as advanced tools to classify textual information in news articles into one or more predefined classes, such as correct or incorrect. Traditional ML methods, such as support vector machine, random forest, and decision tree, are commonly used in news content classification; however, these methods usually require hand-crafted features and struggle with complex text features, thus compromising performance (Minaee et al., 2021).

Along with neural networks being boosted, deep learning frameworks have further enhanced the classification performance by extracting complex content features and capturing nuanced semantic features, such as convolutional neural networks (CNNs) (Kim, 2014; Wang, 2017; Kaliyar et al., 2020), recurrent neural networks (RNNs) (Ma et al., 2016; Ruchansky et al., 2017), and long short-term memory (LSTM) (Sachan et al., 2019; Ma et al., 2020). Kaliyar et al. (Kaliyar et al., 2020) proposed a deep CNN model for incorrect information detection compared to classical CNN and LSTM structures, where it explores pre-trained word embeddings and multiple hidden layers to extract text features.

Additionally, attention networks integrated different features extracted from different latent aspects of news articles to improve detection accuracy (Yang et al., 2016; Linmei et al., 2019; Sun and Lu, 2020; Yun et al., 2023). For example, Yang et al. (Yang et al., 2016) proposed a hierarchical attention network (HAN) to capture the hierarchical structure of documents and employ the word-level and sentence-level attentions. To construct structured graphs based on texts, graph convolutional networks (GCNs) (Yao et al., 2018; Haider Rizvi et al., 2025) have been applied to textual content classification tasks, which construct document-level and corpus-level graphs to learn relationships among words, documents, and corpus.

With the aid of pre-trained knowledge embeddings, the transformer-based models have advanced the detection accuracy of incorrect information in news articles (Croce et al., 2020; Kaliyar et al., 2021; Xiong et al., 2021; Van Nooten and Daelemans, 2025). Combining the bidirectional encoder representations from transformers (BERT) (Devlin

et al., 2019) with a CNN structure, Kaliyar et al. (Kaliyar et al., 2021) proposed a BERT-based incorrect information detection model, where it inputs the BERT embeddings into one-dimensional CNN layers and then detects incorrect information using local features and global dependencies. Along with the data structure and modality extending, multi-modal approaches are proposed to handle more intricate detection tasks for incorrect information content across text, image, video, audio data, or multiple languages (Conneau and Lample, 2019; Abdali et al., 2024; Wu et al., 2024; Lu and Koehn, 2025). For instance, Wu et al. (Wu et al., 2024) emphasized the substantive content over stylistic features, using Large Language Models (LLMs) to reframe news articles and focus on content veracity. Though LLMs emerged with impressive capability of processing multimodal features, LLMs still require a large volume of data to update the known knowledge and maintain performance and reliability.

## 2.2 Knowledge-based methods

Traditional detection methods focus on internal content features and external fact-checking resources to detect incorrect information (Vlachos and Riedel, 2014; Hassan et al., 2015; Guo et al., 2022). For instance, the fact-checking approaches can identify and classify the texts by using the external knowledge sources to fact-check the news content (Etzioni et al., 2008; Wu et al., 2014; Shi and Weninger, 2016; Vo and Lee, 2018). However, these fact-checking approaches are time-consuming and demand human annotations, limiting the scalability and efficiency.

For further exploiting the content and external knowledge features to detect incorrect information, the credibility-based knowledge methods (Popat, 2017; Zhang et al., 2018; Deng et al., 2025) were proposed, which extract the source and content credibility features to identify factual news from non-credible ones, thereby enhancing model performance.

To explore the user behavior, engagements, and interactions on social media, the social relationship-aware approaches (Ghenai and Mejova, 2018; Shu et al., 2019; Dou et al., 2021; Teng et al., 2022) were proposed, which can capture user relationships, news content, and dissemination patterns to improve detection accuracy. For instance, Shu et al. (Shu et al., 2019) presented a tri-relationship-based detection framework of incorrect information con-

tent, where it explores the tri-relationship among publishers, news pieces, and users to differentiate reliable and unreliable articles. Zhang et al. (Zhang et al., 2024) explored the heterogeneous subgraph transformer (HeteroSGT) to detect incorrect information via the heterogeneous graph by unearthing the relationships among news topics, entities, and content.

To understand the propagation patterns of incorrect information within social networks, the network-based methods (Zhou and Zafarani, 2019) were suggested, where these methods focus on the interactions among spreaders and their influence on information propagation. Ma et al. (Ma et al., 2018) presented tree-structured recursive neural networks to model the propagation pattern of tweets for detecting rumors on social media. Typically, graph-based approaches were proposed (Bian et al., 2020b; Fu et al., 2022) to explore the potential of graph structure in modeling social context structures, including knowledge-driven (Wang et al., 2018; Dun et al., 2021), propagation-based (Zhu et al., 2024), and context-aware approaches (Shang et al., 2024; Li et al., 2025).

Another direction of incorrect information detection approaches focuses on enhancing model performance with knowledge generation. Retrieval-augmented methods (Guu et al., 2020; Lewis et al., 2020) apply nearest-neighbor retrieval into LLMs to improve factual reasoning. Though achieving expected performance, these methods are computationally intensive and entangle retrieved knowledge with raw content in an opaque way. In contrast, our model, BiMind, disentangles *content-internal reasoning* from *knowledge-augmented reasoning* within a single yet transparent architecture. This separation strategy allows us to explicitly quantify the value of external knowledge through our proposed uncertainty-aware fusion and VoX metric, which differentiates our model from generic knowledge embedding frameworks.

## 3 Methodology

In this section, we introduce the fundamental framework of our proposed BiMind model, as shown in Figure 2. Here, we define the raw input text  $x_i$  as an internal information unit; all auxiliary information beyond the raw content, such as that retrieved from in-domain memory or linked to external resources, is treated as external knowledge unit. Our objective is to disentangle *content-internal reasoning* from

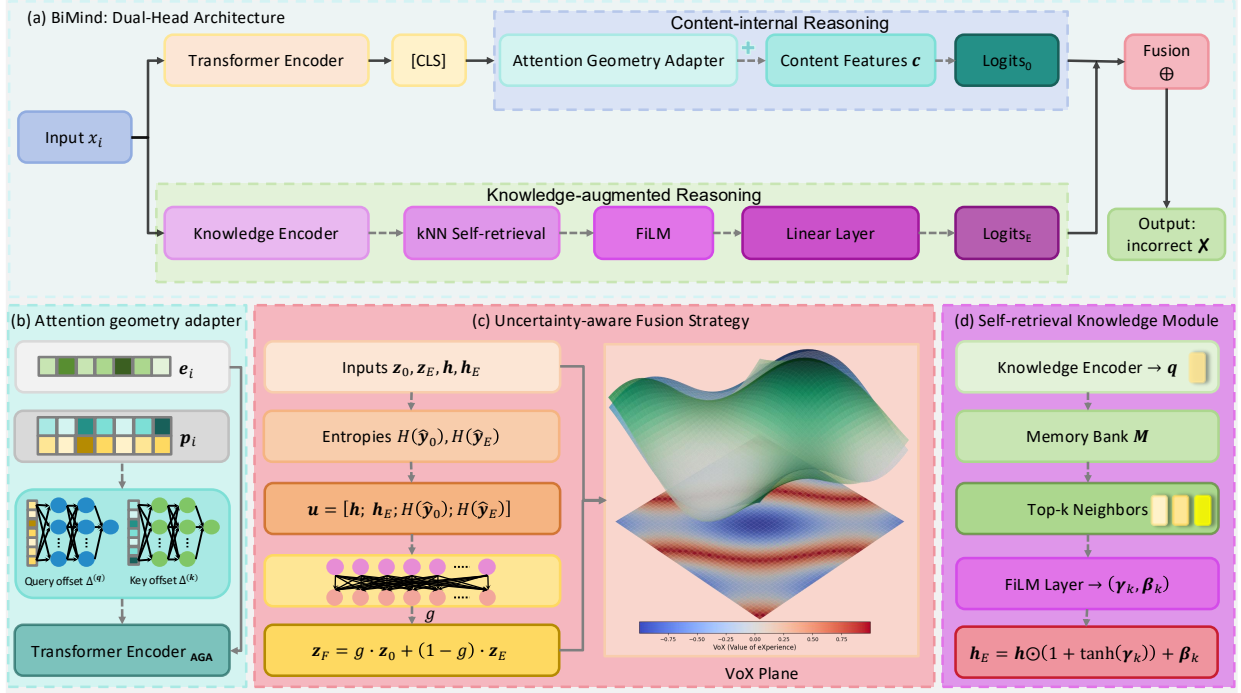


Figure 2: **An illustration of our proposed BiMind framework.** (a) Dual-head architecture with a content-internal head (top) and a knowledge-augmented head (bottom). (b) Attention geometry adapter reshapes pre-softmax attention logits via token-conditioned offsets. (c) Uncertainty-aware fusion combines head logits via an entropy gating, with the VoX metric quantifying the knowledge contributions by comparing head outcomes, where blue and green surfaces in the instance space represent the content and knowledge reasoning heads, respectively. (d) Self-retrieval knowledge module retrieves top- $k$  neighbors and injects knowledge via FiLM to provide knowledge-augmented representations.

267 *knowledge-augmented reasoning* in a structured way, and to provide interpretable diagnostics on  
 268 when and why external knowledge contributes to incorrect information detection. We present **BiMind**,  
 269 a dual-head model with five key ingredients: (1) an attention geometry adapter (AGA) that reshapes  
 270 pre-softmax attention geometry; (2) a self-retrieval knowledge module that constructs an in-domain  
 271 memory through kNN retrieval; (3) a FiLM-based layer that injects retrieved external knowledge into  
 272 the text representations; (4) the uncertainty-aware fusion strategies, including entropy-gated fusion  
 273 and a trainable agreement head, restrained by a symmetric KL regularizer; and (5) a VoX metric  
 274 that quantifies knowledge contributions at the instance level.  
 275  
 276  
 277  
 278  
 279  
 280  
 281  
 282

### 283 3.1 Problem Definitions

284 In this paper, we define the incorrect information detection as assessing whether a given information  
 285 unit  $x_i$  is correct, where  $i$  is the  $i$ -th piece of information. Our detection foundation is that  $x_i$   
 286 is correct if no detected incorrectness exists. Therefore, the detection task is reframed as identifying  
 287  
 288  
 289

incorrect elements within  $x_i$ . Formally, we define: 290

$$291 \quad y(x_i) = \begin{cases} 1 & \text{if } \mathcal{I}(x_i) = \emptyset \\ 0 & \text{otherwise} \end{cases} \quad (1) \quad 292$$

292 Here,  $x_i$  represents title, sentence, article, or narrative.  $\mathcal{I}(x_i)$  is a set of incorrectness identified in  
 293  $x_i$ , such as linguistic elements (tokens or phrases), representation elements (feature embeddings), or  
 294 knowledge elements (retrieved neighbors).  $y(x_i)$  denotes correctness, i.e., 1 (correct information) or  
 295 0 (incorrect information). For incorrect information detection, we model it as a binary classification  
 296 function:  
 297  
 298  
 299  
 300

$$301 \quad f(x_i) \rightarrow y(x_i) \quad (2) \quad 302$$

using a set of labeled training textual data, i.e., 302

$$303 \quad D_{\text{train}} = \{(x_i, y(x_i))\}_{i=1}^{|D_{\text{train}}|} \quad (3) \quad 304$$

304  $y(x_i)$  is the label of  $x_i$ .  $|D_{\text{train}}|$  is the total number of information units in the training dataset. We aim  
 305 at learning the classification function:  
 306

$$307 \quad f(x_i; \theta) = \hat{y}_i \quad (4) \quad 308$$

308 where  $\hat{y}_i \in \{0, 1\}$  denotes the predicted label of  $x_i$  and  $\theta$  is the learnable parameter vector. 309

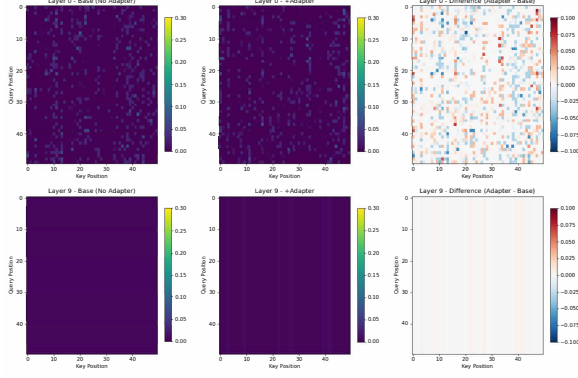


Figure 3: Illustration of the attention maps with (+) and without AGA across shallow (Layer 0) and deep (Layer 9) layers. AGA induces a structured, low-rank attention pattern at deeper layers, reshaping attention distribution by injecting global, key-focused inductive bias.

### 3.2 Attention Geometry Adapter

Let  $x_i = (t_1, t_2, \dots, t_L)$  be a tokenized text sequence.  $t_i$  denotes the  $i$ -th token and  $L$  is the length of the token sequence. Each token  $t_i$  is mapped to an embedding  $e_i \in \mathbb{R}^d$  through an embedding matrix  $\mathbf{E}$ , where  $d$  is the dimension of token embedding:

$$\mathbf{E}(x_i) = [e_1, e_2, \dots, e_L] \in \mathbb{R}^{L \times d} \quad (5)$$

Instead of directly modifying token embeddings, we introduce an AGA module that reshapes attention distributions at the pre-softmax logit level. For each token  $t_i$ , we assign a token-level attribute vector  $\mathbf{p}_i \in \{0, 1\}^{D_{pos}}$  by using part-of-speech (POS) categories, where  $D_{pos}$  is the number of POS tags. In our POS tag set, we set  $D_{pos} = 5$ , including VERB/AUX, NOUN, ADJ, ADV, and OTHER. This representation provides an interpretable, low-dimensional basis for conditioning attention geometry, where attention geometry denotes the structural properties of attention distributions across tokens, beyond individual attention weights.

Then, the Transformer encoder projects token embeddings  $\mathbf{E}(x_i)$  into queries, keys, and values as in the standard self-attention. For each attention head  $h$ , AGA computes token-conditioned logit offsets  $\Delta$  of query and key via lightweight multilayer perceptrons (MLPs):

$$\Delta^{(q)} = f_q(\mathbf{p}_i), \quad \Delta^{(k)} = f_k(\mathbf{p}_i) \quad (6)$$

where  $f_q(\cdot)$  and  $f_k(\cdot)$  are two-layer MLPs. The final pre-softmax attention logits are updated as:

$$\tilde{\mathbf{A}}_{i,j}^{(h)} = \frac{\mathbf{q}_i^{(h)\top} \mathbf{k}_j^{(h)}}{\sqrt{d_k}} + \Delta_{h,i}^{(q)} + \Delta_{h,j}^{(k)}, \quad (7)$$

where  $\tilde{\mathbf{A}}_{i,j}^{(h)}$  denotes the pre-softmax attention logit between query token  $i$  and key token  $j$  in attention head  $h$ ;  $\mathbf{q}_i^{(h)}$  and  $\mathbf{k}_j^{(h)}$  denote the  $i$ -th query and  $j$ -th key representations projected from  $\mathbf{E}(x_i)$ ;  $d_k$  is the dimension of the key vectors;  $\Delta_{h,i}^{(q)}$  and  $\Delta_{h,j}^{(k)}$  are token-conditioned offsets for head  $h$  applied to the query and key logits, respectively. More details of AGA are provided in the Appendix.

By injecting structured offsets, AGA reshapes the attention distributions, increasing entropy and mitigating attention collapse while leaving token embeddings unchanged, as shown in Figure 3. The attention outputs are then computed following standard multi-head attention and passed through the Transformer encoder  $\mathcal{T}_{AGA}(\cdot)$ :

$$\mathbf{H}_i = \mathcal{T}_{AGA}(\mathbf{E}(x_i)) \in \mathbb{R}^{L \times d} \quad (8)$$

in which  $\mathbf{H}_i$  is the sequence representation. Finally, we apply max-pooling to capture the most salient features  $\mathbf{h}$  in the sequence:

$$\mathbf{h} = \max_{i=1}^L \mathbf{H}_i \in \mathbb{R}^d \quad (9)$$

### 3.3 Semantic Neighbor Retrieval

In this section, we construct an in-domain semantic memory  $\mathbf{M} = \{\mathbf{m}_1, \mathbf{m}_2, \dots, \mathbf{m}_N\}$  by encoding all training information units with a pre-trained LLaMA-7B (Touvron et al., 2023).  $\mathbf{m}_j \in \mathbb{R}^{d_s}$  is the embedding of one information unit, normalized to unit length.  $d_s$  is the dimension of Sentence-Transformer embeddings, and  $N$  is the number of training units stored in  $\mathbf{M}$ . For an input  $x_i$ , we encode it as query  $\mathbf{q} \in \mathbb{R}^{d_s}$  and compute cosine similarity  $s_i$  between  $\mathbf{q}$  and  $\mathbf{m}$ :

$$s_j = \mathbf{q}^\top \mathbf{m}_j, \quad j = 1, \dots, N \quad (10)$$

Next, we select the top- $k$  neighbors with indices  $\mathcal{N}(x_i)$  and aggregate:

$$\bar{\mathbf{m}} = \frac{1}{k} \sum_{j \in \mathcal{N}(x_i)} \mathbf{m}_j. \quad (11)$$

To inject retrieved knowledge neighbors, we map  $\bar{\mathbf{m}}$  into modulation parameters  $\gamma_k$  and  $\beta_k$ :

$$\gamma_k = \mathbf{W}_\gamma \bar{\mathbf{m}} + \mathbf{b}_\gamma, \quad \beta_k = \mathbf{W}_\beta \bar{\mathbf{m}} + \mathbf{b}_\beta \quad (12)$$

Here,  $\mathbf{W}_\gamma, \mathbf{W}_\beta \in \mathbb{R}^{d \times d_s}$  are projection matrices;  $\mathbf{b}_\gamma$  and  $\mathbf{b}_\beta$  are bias terms. We then apply FiLM (Perez et al., 2018) to produce the knowledge-augmented representation  $\mathbf{h}_E$ :

$$\mathbf{h}_E = \mathbf{h} \odot (1 + \tanh(\gamma_k)) + \beta_k \quad (13)$$

where  $\odot$  is element-wise multiplication. Film adaptively scales  $(1 + \tanh(\gamma_k))$  and shifts  $(\beta_k)$  each dimension of  $\mathbf{h}$  based on knowledge retrieved from semantic memory, creating a knowledge-augmented representation  $\mathbf{h}_E$ .

### 3.4 Dual-head Prediction

Combining text representations with content features  $\mathbf{c} \in \mathbb{R}^{d_c}$ , we define two reasoning heads:

$$\mathbf{z}_0 = \mathbf{W}_0[\mathbf{h}; \mathbf{c}] + \mathbf{b}_0, \quad \mathbf{z}_E = \mathbf{W}_E[\mathbf{h}_E; \mathbf{c}] + \mathbf{b}_E \quad (14)$$

where  $\mathbf{z}_0$  and  $\mathbf{z}_E \in \mathbb{R}^K$  are the outputs of the content-internal and knowledge-augmented reasoning heads, respectively.  $K$  is the number of labels.  $\mathbf{W}_0, \mathbf{W}_E \in \mathbb{R}^{d \times (d+d_c)}$  are projection matrices;  $\mathbf{b}_0$  and  $\mathbf{b}_E$  are bias terms. Then,  $\mathbf{z}_0, \mathbf{z}_E$  are transformed into probability distributions through softmax:

$$\hat{\mathbf{y}}_0 = \text{softmax}(\mathbf{z}_0), \quad \hat{\mathbf{y}}_E = \text{softmax}(\mathbf{z}_E) \quad (15)$$

$\hat{\mathbf{y}}_0$  is the prediction result from content-internal reasoning Head<sub>0</sub>, and it's what the model "believes" without external knowledge. Head<sub>E</sub> reflects knowledge-augmented reasoning and derives  $\hat{\mathbf{y}}_E$ , and  $\hat{\mathbf{y}}_E$  is what the model "believes" with knowledge. Together, we can explore how knowledge affects predictions.

### 3.5 Uncertainty-aware Fusion Strategy

We fuse two predictions from Head<sub>0</sub> and Head<sub>E</sub> using an entropy-gated strategy and a trainable agreement head, respectively. Using the entropy-gated fusion strategy, we first compute entropy for each head:

$$\mathcal{H}(\hat{\mathbf{y}}) = - \sum_{k=1}^K \hat{y}_k \log \hat{y}_k \quad (16)$$

Then, we formulate the gate input vector  $\mathbf{u}$ , and feed it into MLP gate:

$$g = \sigma(\mathbf{W}_g \mathbf{u} + \mathbf{b}_g) \in (0, 1) \quad (17)$$

$g$  is the fusion weight.  $\mathbf{W}_g$  and  $\mathbf{b}_g$  are parameters of the MLP gate. Finally, we fuse logits:

$$\mathbf{z}_F = g \cdot \mathbf{z}_0 + (1 - g) \cdot \mathbf{z}_E, \quad \hat{\mathbf{y}}_F = \text{softmax}(\mathbf{z}_F) \quad (18)$$

where  $\mathbf{z}_F$  is the fused logits combining content-internal and knowledge-augmented reasoning.  $\hat{\mathbf{y}}_F$  is the final prediction results. Therefore, if Head<sub>0</sub> has high entropy (uncertainty), the gate shifts the weight toward Head<sub>E</sub>, and vice versa. More details can be found in the Appendix.

### 3.6 Agreement Regularization

To stabilize training, we enforce the agreement between heads while preserving differences. We define the symmetric KL regularizer as:

$$\mathcal{L}_{\text{agree}}^{(i)} = \frac{1}{2} \left[ D_{\text{KL}}(\hat{\mathbf{y}}_0^{(i)} \parallel \hat{\mathbf{y}}_E^{(i)}) + D_{\text{KL}}(\hat{\mathbf{y}}_E^{(i)} \parallel \hat{\mathbf{y}}_0^{(i)}) \right] \quad (19)$$

where  $\mathcal{L}_{\text{agree}}^{(i)}$  is agreement loss.  $D_{\text{KL}}(\hat{\mathbf{y}}_0^{(i)} \parallel \hat{\mathbf{y}}_E^{(i)})$  is the KL divergence between distributions  $\hat{\mathbf{y}}_0^{(i)}$  and  $\hat{\mathbf{y}}_E^{(i)}$ . Based on the symmetric KL regularizer, our training objective is:

$$\mathcal{L} = \frac{1}{n} \sum_{i=1}^n \left[ \mathcal{L}_{\text{CE}}(\mathbf{z}_F^{(i)}, y(x_i)) + \frac{1}{2} \mathcal{L}_{\text{CE}}(\mathbf{z}_0^{(i)}, y(x_i)) + \frac{1}{2} \mathcal{L}_{\text{CE}}(\mathbf{z}_E^{(i)}, y(x_i)) + \lambda \mathcal{L}_{\text{agree}}^{(i)} \right] \quad (20)$$

where  $\mathcal{L}_{\text{CE}}^{(i)}$  is cross-entropy (CE) loss, and  $\lambda$  is the agreement loss weight. Through the loss function  $\mathcal{L}$ , we encourage both heads to produce consistent predictions while maintaining their distinct reasoning.

### 3.7 Value-of-experience Metric

To measure knowledge contributions, we define VoX at the instance level. Terminologically, we refer to the retrieved knowledge as "experience" in our framework, to clarify its role as external evidence augmenting content-internal predictions. Given the correctness label  $y(x_i)$ , VoX is:

$$\text{VoX}(x_i) = \mathbf{z}_E[y(x_i)] - \mathbf{z}_0[y(x_i)]. \quad (21)$$

Our interpretations are summarized as follows:

- $\text{VoX}(x_i) > 0$ : knowledge increases confidence in correct class.
- $\text{VoX}(x_i) < 0$ : knowledge decreases confidence, suggesting potential noise.
- $\text{VoX}(x_i) \approx 0$ : knowledge has little effect.

Unlike raw accuracy or F1 score, VoX highlights *when and why* knowledge matters and provides interpretable diagnostics on knowledge augmentation.

## 4 Experiments

In this section, we conducted extensive experiments on four public datasets collected from real-world scenarios, and experimental results demonstrate that our model has superior performance

and efficiency to most tested models. We first introduced the experimental setup, including the datasets, tested models, and experimental settings. Then, we reported the experiment results and VoX values, and then analyzed these results for further exploration. Furthermore, the ablation study shows the modules contributing to the performance improvement. More details are provided in the Appendix.

#### 4.1 Experimental Setup

**Datasets.** For conducting the extensive experiments, we used four datasets to broadly test our model and other advanced models, including health datasets (MM COVID (Li et al., 2020) and ReCOVery (Zhou et al., 2020)), news content dataset (LIAR (Wang, 2017)), and multi-domain dataset (MC Fake (Min et al., 2022)).

**Experimental Models.** To fairly perform the comparison experiments, we compared our proposed BiMind model with five models, which include a CNN-based model (Kim, 2014), a GCN-based model (Yao et al., 2018), HAN (Yang et al., 2016), BERT (Devlin et al., 2019), and HeteroSGT (Zhang et al., 2024).

#### 4.2 Experiment Settings

For training and testing our proposed model, we split all the datasets into train, validation, and test datasets using a ratio of 80%, 10%, and 10%, respectively. To validate the generalizability of tested methods, we performed 10 rounds of tests with random seeds for each model and then recorded the average results and standard deviation. Here, all the experiments were conducted on 1 NVIDIA A100 GPU with 40 G RAM. We quantitatively evaluated our model’s performance compared to the other five tested models, using classification metrics such as accuracy (Acc), Macro-precision (Pre), Macro-F1 (F1), and Macro-recall (Rec).

#### 4.3 Experimental Results

In Table 1, we reported the experimental results of all the tested models across the four datasets. From Table 1, one can see that our model achieves superior performance across all the metrics on the MM COVID, LIAR, and ReCOVery datasets, and suboptimal performance on the dataset MC Fake. It shows that our modules can improve the model performance and have a significant impact on detecting incorrect information. Additionally, we can see that our model achieves higher recall values

on all four datasets, typically on the MM COVID, LIAR, and ReCOVery datasets. A higher recall indicates that less incorrect information is missed. Furthermore, it should be noted that our model has robust and consistent performance across all the datasets, compared with other tested models. Though HeteroSGT achieves the optimal results, such as Rec and F1 on MC Fake due to its subgraph structure, it still drops performance by 19.1% on Acc and 19.1% on Pre, 5.2% on Acc and 5.7% on Pre, respectively, compared to our proposed model on ReCOVery and LIAR datasets. More details are provided in the Appendix.

#### 4.4 Case Study

As illustrated in Table 2, the performance of BiMind varies across benchmark datasets due to the gate routes between  $Head_0$  and  $Head_E$ . On datasets ReCOVery (+0.47 / 84.24% VoX,  $\approx 0.04$  Gate) and MM COVID (+0.97 / 83.29% VoX,  $\approx 0.03$  Gate), the gate leans strongly towards  $Head_E$  because the retrieved knowledge positively aligned with ground-truth labels. On MC Fake ( $-0.08$  / 39.91% VoX,  $\approx 0.22$  Gate), the fusion has partial reliance on knowledge and generates mixed results, which improve minority-class recall but introduce noise. In contrast, on LIAR (+0.07 / 60.56% VoX,  $\approx 0.19$  Gate), we can see that when external knowledge is noisy, it leads fusion to weaken the predictions with a significant drop in F1 (58.78  $\rightarrow$  47.30), highlighting that low gate values are not always effective and thus must be interpreted in the context of knowledge integrity and veracity. Additional analysis can be found in the Appendix.

#### 4.5 Ablation Study

We conducted an ablation study on the ReCOVery dataset to evaluate the performance of four core modules in our model: AGA, self-retrieved knowledge module via FiLM, fusion strategies (entropy-gated scheme and trainable agreement head), and symmetric KL regularizer. From Table 3, we can see that the BiMind model, with all these four modules, achieved the best performance, i.e., Acc of 0.897, Pre of 0.895, Rec of 0.897, and F1 score of 0.895. More results can be found in the Appendix.

### 5 Limitations

Though our proposed BiMind framework has superior performance in the incorrect information detection task by integrating textual and knowledge features, several limitations remain. First, AGA condi-

Table 1: Detection performance on four datasets (best in red, second-best in blue).

Dataset	CNN		GCN		BERT		HAN		HeteroSGT		BiMind	
	Acc	Pre	Acc	Pre	Acc	Pre	Acc	Pre	Acc	Pre	Acc	Pre
MM COVID	0.582±0.035	0.478±0.170	0.717±0.156	0.735±0.236	0.730±0.093	0.727±0.094	0.855±0.005	0.854±0.005	0.915±0.009	0.905±0.011	0.951±0.008	0.950±0.011
ReCOVery	0.658±0.011	0.460±0.104	0.718±0.037	0.691±0.178	0.682±0.030	0.441±0.213	0.722±0.021	0.462±0.197	0.727±0.023	0.731±0.047	0.918±0.013	0.922±0.013
MC Fake	0.825±0.001	0.544±0.156	0.724±0.138	0.516±0.169	0.827±0.006	0.713±0.271	0.825±0.005	0.463±0.098	0.883±0.002	0.812±0.003	0.887±0.005	0.827±0.006
LIAR	0.546±0.019	0.432±0.181	0.487±0.039	0.493±0.047	0.537±0.007	0.513±0.017	0.546±0.025	0.493±0.036	0.581±0.002	0.580±0.003	0.633±0.001	0.637±0.002
Dataset	Rec	F1	Rec	F1	Rec	F1	Rec	F1	Rec	F1	Rec	F1
MM COVID	0.547±0.039	0.474±0.101	0.685±0.178	0.621±0.184	0.722±0.101	0.720±0.103	0.854±0.006	0.853±0.005	0.883±0.013	0.893±0.011	0.951±0.009	0.951±0.008
ReCOVery	0.501±0.020	0.422±0.107	0.609±0.102	0.516±0.021	0.722±0.081	0.416±0.032	0.506±0.002	0.457±0.013	0.585±0.036	0.571±0.049	0.918±0.013	0.919±0.013
MC Fake	0.501±0.002	0.455±0.004	0.552±0.169	0.470±0.039	0.502±0.001	0.451±0.002	0.500±0.004	0.453±0.001	0.762±0.002	0.783±0.003	0.700±0.099	0.738±0.109
LIAR	0.502±0.005	0.377±0.049	0.494±0.029	0.423±0.055	0.510±0.012	0.483±0.014	0.502±0.018	0.445±0.053	0.575±0.002	0.571±0.003	0.636±0.003	0.633±0.002

Table 2: Cross-dataset VoX results. Metrics are Acc, F1, Pre, and Rec. We report mean VoX value and percentage of samples with positive gain (pos%); we also show mean gate value and routing mass below/above thresholds, with %<0.3 indicating the gate leaned strongly toward knowledge head Head<sub>E</sub>, and %>0.7 indicating it leaned strongly toward content head Head<sub>0</sub>.

Dataset	Head/Mode	Acc	F1	Pre	Rec	VoX (mean / pos%)	Gate mean (%<0.3 / %>0.7)
ReCOVery	Head <sub>0</sub>	85.22	85.15	85.10	85.22	–	–
	Head <sub>E</sub>	87.19	86.93	86.98	87.19	+0.47 / 84.24%	0.04 (100.00% / 0.00%)
	Fused	87.19	86.93	86.98	87.19	–	0.04 (100.00% / 0.00%)
MC Fake	Head <sub>0</sub>	86.50	84.85	84.79	86.50	–	–
	Head <sub>E</sub>	87.35	86.90	86.63	87.35	-0.08 / 39.91%	0.22 (81.24% / 0.00%)
	Fused	87.42	86.82	86.52	87.42	–	0.22 (81.24% / 0.00%)
MM COVID	Head <sub>0</sub>	81.70	81.78	82.13	81.70	–	–
	Head <sub>E</sub>	90.45	90.51	91.18	90.45	+0.97 / 83.29%	0.03 (100.00% / 0.00%)
	Fused	90.72	90.77	91.38	90.72	–	0.03 (100.00% / 0.00%)
LIAR	Head <sub>0</sub>	59.90	58.78	59.66	59.90	–	–
	Head <sub>E</sub>	57.70	47.30	66.32	57.70	+0.07 / 60.56%	0.19 (100.00% / 0.00%)
	Fused	58.29	48.66	66.51	58.29	–	0.19 (100.00% / 0.00%)

Table 3: Ablation study on ReCOVery dataset. We remove one module at a time from the full BiMind model and report Acc, Pre, Rec, and F1.

Model Variant	Acc	Pre	Rec	F1
Full BiMind model (w/ knowledge)	<b>0.897</b>	<b>0.895</b>	<b>0.897</b>	<b>0.895</b>
Baseline (content w/o knowledge)	0.852	0.849	0.852	0.848
– Attention geometry adapter	0.872	0.870	0.872	0.870
– Knowledge retrieval	0.847	0.847	0.847	0.847
– Gated fusion	0.862	0.861	0.862	0.861
– Trainable agreement head	0.867	0.868	0.867	0.867
– Symmetric KL Regularizer	0.872	0.881	0.872	0.874

tions attention geometry on token-level attributes, which might be less efficient for inputs with limited salient lexical signals. Secondly, BiMind does not incorporate social credibility or propagation patterns into the detection pipeline. Then, when the detection model has prediction errors, it might weaken the correct information flow.

## 6 Conclusion

Incorrect information significantly disrupts content quality and integrity on social media platforms, and therefore, it’s increasingly important to develop de-

tection models that are efficient and interpretable. Compared to most detection approaches that blend textual content and external knowledge, we proposed **BiMind**, a dual-head framework that explicitly disentangles *content-internal reasoning* from *knowledge-augmented reasoning* for incorrect information detection. In this work, we first designed an attention geometry adapter that reshapes attention distributions to prevent attention collapse. Secondly, an in-memory semantic knowledge base was constructed to retrieve and encode external knowledge features through the FiLM layer. Then, we introduced two uncertainty-aware fusion strategies, including an entropy-gated scheme and a trainable agreement head, regularized by a symmetric KL regularizer. Finally, we defined the VoX metric, which quantifies the knowledge contributions, providing interpretable diagnostics at the instance level on *when* and *why* knowledge impacts detection. Experimental results across benchmark datasets show that BiMind achieves competitive performance while providing interpretable insights on knowledge injections.

## References

- Sara Abdali, Sina Shaham, and Bhaskar Krishnamachari. 2024. [Multi-modal misinformation detection: Approaches, challenges and opportunities](#). *ACM Computing Surveys*, 57(3):1–29.
- Sajjad Ahmed, Knut Hinkelmann, and Flavio Corradini. 2022. [Combining machine learning with knowledge engineering to detect fake news in social networks—a survey](#). *ArXiv*, abs/2201.08032.
- Bimal Bhattarai, Ole-Christoffer Granmo, and Lei Jiao. 2021. [Explainable tsetlin machine framework for fake news detection with credibility score assessment](#). *ArXiv*, abs/2105.09114.
- Tian Bian, Xi Xiao, Tingyang Xu, Peilin Zhao, Wenbing Huang, Yu Rong, and Junzhou Huang. 2020a. [Rumor detection on social media with bi-directional graph convolutional networks](#). *Proceedings of the AAAI Conference on Artificial Intelligence*, 34(01):549–556.
- Tian Bian, Xi Xiao, Tingyang Xu, Peilin Zhao, Wenbing Huang, Yu Rong, and Junzhou Huang. 2020b. [Rumor detection on social media with bi-directional graph convolutional networks](#). In *Proceedings of the AAAI Conference on Artificial Intelligence*, volume 34, pages 549–556.
- Alexis Conneau and Guillaume Lample. 2019. [Cross-lingual language model pretraining](#). In *Proceedings of the 33rd International Conference on Neural Information Processing Systems*, pages 7059–7069.
- Danilo Croce, Giuseppe Castellucci, and Roberto Basili. 2020. [GAN-BERT: Generative adversarial learning for robust text classification with a bunch of labeled examples](#). In *Proceedings of the 58th Annual Meeting of the Association for Computational Linguistics*, pages 2114–2119, Online. Association for Computational Linguistics.
- Boyi Deng, Wenjie Wang, Fengbin Zhu, Qifan Wang, and Fuli Feng. 2025. [Cram: Credibility-aware attention modification in llms for combating misinformation in rag](#). In *Proceedings of the AAAI Conference on Artificial Intelligence*, volume 39, pages 23760–23768.
- Jacob Devlin, Ming-Wei Chang, Kenton Lee, and Kristina Toutanova. 2019. [Bert: Pre-training of deep bidirectional transformers for language understanding](#). In *Proceedings of the 2019 Conference of the North American Chapter of the Association for Computational Linguistics: Human Language Technologies, volume 1 (long and short papers)*, pages 4171–4186.
- Yingtong Dou, Kai Shu, Congying Xia, Philip S. Yu, and Lichao Sun. 2021. [User preference-aware fake news detection](#). In *Proceedings of the 44th International ACM SIGIR Conference on Research and Development in Information Retrieval*, SIGIR ’21, page 2051–2055, New York, NY, USA. Association for Computing Machinery.
- Yaqian Dun, Kefei Tu, Chen Chen, Chunyan Hou, and Xiaojie Yuan. 2021. [Kan: Knowledge-aware attention network for fake news detection](#). In *Proceedings of the AAAI Conference on Artificial Intelligence*, volume 35, pages 81–89.
- Oren Etzioni, Michele Banko, Stephen Soderland, and Daniel S Weld. 2008. [Open information extraction from the web](#). *Communications of the ACM*, 51(12):68–74.
- Dongqi Fu, Yikun Ban, Hanghang Tong, Ross Maciejewski, and Jingrui He. 2022. [Disco: Comprehensive and explainable disinformation detection](#). *Proceedings of the 31st ACM International Conference on Information & Knowledge Management*, pages 4848–4852.
- Amira Ghenai and Yelena Mejova. 2018. [Fake cures: user-centric modeling of health misinformation in social media](#). In *Proceedings of the ACM on Human-Computer Interaction*, volume 2, pages 1–20. ACM New York, NY, USA.
- Bin Guo, Yasan Ding, Lina Yao, Yunji Liang, and Zhiwen Yu. 2020. [The future of false information detection on social media: New perspectives and trends](#). *ACM Computing Survery*, 53(4).
- Zhijiang Guo, Michael Schlichtkrull, and Andreas Vlachos. 2022. [A survey on automated fact-checking](#). *Transactions of the Association for Computational Linguistics*, 10:178–206.
- Kelvin Guu, Kenton Lee, Zora Tung, Panupong Pasupat, and Ming-Wei Chang. 2020. [Realm: retrieval-augmented language model pre-training](#). In *Proceedings of the 37th International Conference on Machine Learning*, ICML’20. JMLR.org.
- Syed Mustafa Haider Rizvi, Ramsha Imran, and Arif Mahmood. 2025. [Text classification using graph convolutional networks: A comprehensive survey](#). *ACM Computing Survery*, 57(8).
- Naeemul Hassan, Chengkai Li, and Mark Tremayne. 2015. [Detecting check-worthy factual claims in presidential debates](#). In *Proceedings of the 24th ACM International on Conference on Information and Knowledge Management*, CIKM ’15, page 1835–1838, New York, NY, USA. Association for Computing Machinery.
- Pengcheng He, Xiaodong Liu, Jianfeng Gao, and Weizhu Chen. 2020. [Deberta: Decoding-enhanced bert with disentangled attention](#). *arXiv preprint arXiv:2006.03654*.
- Ammar Ismael Kadhim. 2019. [Survey on supervised machine learning techniques for automatic text classification](#). *Artificial Intelligence Review*, 52:273–292.
- Rohit Kumar Kaliyar, Anurag Goswami, and Pratik Narang. 2021. [Fakebert: Fake news detection in social media with a bert-based deep learning approach](#). *Multimedia tools and applications*, 80(8):11765–11788.

711	Rohit Kumar Kaliyar, Anurag Goswami, Pratik Narang, and Soumendu Sinha. 2020. <a href="#">Fndnet—a deep convolutional neural network for fake news detection</a> . <i>Cognitive Systems Research</i> , 61:32–44.	768
712		769
713		770
714		771
715	Yoon Kim. 2014. <a href="#">Convolutional neural networks for sentence classification</a> . In <i>Proceedings of the 2014 Conference on Empirical Methods in Natural Language Processing</i> , pages 1746–1751, Doha, Qatar. Association for Computational Linguistics.	772
716		773
717		774
718		775
719		776
720	Patrick Lewis, Ethan Perez, Aleksandra Piktus, Fabio Petroni, Vladimir Karpukhin, Naman Goyal, Heinrich Küttler, Mike Lewis, Wen-tau Yih, Tim Rocktäschel, Sebastian Riedel, and Douwe Kiela. 2020. Retrieval-augmented generation for knowledge-intensive nlp tasks. In <i>Proceedings of the 34th International Conference on Neural Information Processing Systems, NIPS ’20</i> , Red Hook, NY, USA. Curran Associates Inc.	777
721		778
722		779
723		780
724		781
725		782
726		783
727		784
728		785
729	Guoyi Li, Die Hu, Zongzhen Liu, Xiaodan Zhang, and Honglei Lyu. 2025. <a href="#">Semantic reshuffling with LLM and heterogeneous graph auto-encoder for enhanced rumor detection</a> . In <i>Proceedings of the 31st International Conference on Computational Linguistics</i> , pages 8557–8572, Abu Dhabi, UAE. Association for Computational Linguistics.	786
730		787
731		788
732		789
733		790
734		791
735		792
736	Yichuan Li, Bohan Jiang, Kai Shu, and Huan Liu. 2020. <a href="#">Mm-covid: A multilingual and multimodal data repository for combating covid-19 disinformation</a> . <i>ArXiv</i> , abs/2011.04088.	793
737		794
738		795
739		796
740	Hu Linmei, Tianchi Yang, Chuan Shi, Houye Ji, and Xiaoli Li. 2019. <a href="#">Heterogeneous graph attention networks for semi-supervised short text classification</a> . In <i>Proceedings of the 2019 Conference on Empirical Methods in Natural Language Processing and the 9th International Joint Conference on Natural Language Processing</i> , pages 4821–4830, Hong Kong, China. Association for Computational Linguistics.	797
741		798
742		799
743		800
744		801
745		802
746		803
747		804
748	Yinhan Liu, Myle Ott, Naman Goyal, Jingfei Du, Mandar Joshi, Danqi Chen, Omer Levy, Mike Lewis, Luke Zettlemoyer, and Veselin Stoyanov. 2019. Roberta: A robustly optimized bert pretraining approach. <i>arXiv preprint arXiv:1907.11692</i> .	805
749		806
750		807
751		808
752		809
753	TaiMing Lu and Philipp Koehn. 2025. <a href="#">Learn and unlearn: Addressing misinformation in multilingual LLMs</a> . In <i>Proceedings of the 2025 Conference on Empirical Methods in Natural Language Processing</i> , pages 10191–10206, Suzhou, China. Association for Computational Linguistics.	810
754		811
755		812
756		813
757		814
758		815
759	Jing Ma, Wei Gao, Prasenjit Mitra, Sejeong Kwon, Bernard J. Jansen, Kam-Fai Wong, and Meeyoung Cha. 2016. <a href="#">Detecting rumors from microblogs with recurrent neural networks</a> . In <i>Proceedings of the Twenty-Fifth International Joint Conference on Artificial Intelligence, IJCAI’16</i> , page 3818–3824. AAAI Press.	816
760		817
761		818
762		819
763		820
764		821
765		822
766	Jing Ma, Wei Gao, and Kam-Fai Wong. 2018. <a href="#">Rumor detection on Twitter with tree-structured recursive neural networks</a> . In <i>Proceedings of the 56th Annual Meeting of the Association for Computational Linguistics (Volume 1: Long Papers)</i> , pages 1980–1989, Melbourne, Australia. Association for Computational Linguistics.	823
767		824
		825
	Qianli Ma, Zhenxi Lin, Jiangyue Yan, Zipeng Chen, and Liuhong Yu. 2020. <a href="#">MODE-LSTM: A parameter-efficient recurrent network with multi-scale for sentence classification</a> . In <i>Proceedings of the 2020 Conference on Empirical Methods in Natural Language Processing</i> , pages 6705–6715, Online. Association for Computational Linguistics.	
	Valeria Mazzeo, Andrea Rapisarda, and Giovanni Giuffrida. 2021. <a href="#">Detection of fake news on covid-19 on web search engines</a> . <i>Frontiers in Physics</i> , 9:685730.	
	Erxue Min, Yu Rong, Yatao Bian, Tingyang Xu, Peilin Zhao, Junzhou Huang, and Sophia Ananiadou. 2022. <a href="#">Divide-and-conquer: Post-user interaction network for fake news detection on social media</a> . In <i>Proceedings of the ACM Web Conference 2022, WWW ’22</i> , page 1148–1158, New York, NY, USA. Association for Computing Machinery.	
	Shervin Minaee, Nal Kalchbrenner, Erik Cambria, Narjes Nikzad, Meysam Chenaghlu, and Jianfeng Gao. 2021. <a href="#">Deep learning-based text classification: A comprehensive review</a> . <i>ACM Computing Survery</i> , 54(3).	
	Ethan Perez, Florian Strub, Harm De Vries, Vincent Dumoulin, and Aaron Courville. 2018. <a href="#">Film: Visual reasoning with a general conditioning layer</a> . In <i>Proceedings of the AAAI conference on artificial intelligence</i> , volume 32.	
	Kashyap Popat. 2017. <a href="#">Assessing the credibility of claims on the web</a> . In <i>Proceedings of the 26th International Conference on World Wide Web Companion, WWW ’17 Companion</i> , page 735–739, Republic and Canton of Geneva, CHE. International World Wide Web Conferences Steering Committee.	
	Natali Ruchansky, Sungyong Seo, and Yan Liu. 2017. <a href="#">Csi: A hybrid deep model for fake news detection</a> . In <i>Proceedings of the 2017 ACM on Conference on Information and Knowledge Management, CIKM ’17</i> , page 797–806, New York, NY, USA. Association for Computing Machinery.	
	Devendra Singh Sachan, Manzil Zaheer, and Ruslan Salakhutdinov. 2019. <a href="#">Revisiting lstm networks for semi-supervised text classification via mixed objective function</a> . In <i>Proceedings of the AAAI Conference on Artificial Intelligence</i> , volume 33, pages 6940–6948.	
	Lanyu Shang, Yang Zhang, Bozhang Chen, Ruohan Zong, Zhenrui Yue, Huimin Zeng, Na Wei, and Dong Wang. 2024. <a href="#">Mmadapt: A knowledge-guided multi-source multi-class domain adaptive framework for early health misinformation detection</a> . In <i>Proceedings of the ACM Web Conference 2024, WWW ’24</i> , page 4653–4663, New York, NY, USA. Association for Computing Machinery.	



936	Chang Yang, Peng Zhang, Wenbo Qiao, Hui Gao, and	<a href="#">Rumor detection on social media with crowd intelligence and ChatGPT-assisted networks</a> . In <i>Proceedings of the 2023 Conference on Empirical Methods in Natural Language Processing</i> , pages 5705–5717, Singapore. Association for Computational Linguistics.	
937	Jiaming Zhao. 2023.		
938			
939			
940			
941			
942			
943	Zichao Yang, Diyi Yang, Chris Dyer, Xiaodong He,	<a href="#">Hierarchical attention networks for document classification</a> . In <i>Proceedings of the 2016 Conference of the North American Chapter of the Association for Computational Linguistics: Human Language Technologies</i> , pages 1480–1489, San Diego, California. Association for Computational Linguistics.	
944	Alex Smola, and Eduard Hovy. 2016.		
945			
946			
947			
948			
949			
950			
951	Liang Yao, Chengsheng Mao, and Yuan Luo. 2018.	<a href="#">Graph convolutional networks for text classification</a> . <i>ArXiv</i> , abs/1809.05679.	
952			
953			
954	Jungmin Yun, Mihyeon Kim, and Youngbin Kim. 2023.	<a href="#">Focus on the core: Efficient attention via pruned token compression for document classification</a> . In <i>Findings of the Association for Computational Linguistics: EMNLP 2023</i> , pages 13617–13628, Singapore. Association for Computational Linguistics.	
955			
956			
957			
958			
959			
960	Amy X. Zhang, Aditya Ranganathan, Sarah Emlen	<a href="#">A structured response to misinformation: Defining and annotating credibility indicators in news articles</a> . In <i>Companion Proceedings of the The Web Conference 2018</i> , WWW '18, page 603–612, Republic and Canton of Geneva, CHE. International World Wide Web Conferences Steering Committee.	
961	Metz, Scott Appling, Connie Moon Sehat, Norman		
962	Gilmore, Nick B. Adams, Emmanuel Vincent, Jen-		
963	nifer Lee, Martin Robbins, Ed Bice, Sandro Hawke,		
964	David Karger, and An Xiao Mina. 2018.		
965			
966			
967			
968			
969			
970			
971	Yuchen Zhang, Xiaoxiao Ma, Jia Wu, Jian Yang, and	<a href="#">Heterogeneous subgraph transformer for fake news detection</a> . In <i>Proceedings of the ACM Web Conference 2024</i> , WWW '24, page 1272–1282, New York, NY, USA. Association for Computing Machinery.	
972	Hao Fan. 2024.		
973			
974			
975			
976			
977	Xinyi Zhou, Apurva Mulay, Emilio Ferrara, and Reza	<a href="#">Recovery: A multimodal repository for covid-19 news credibility research</a> . In <i>Proceedings of the 29th ACM International Conference on Information &amp; Knowledge Management</i> , CIKM '20, page 3205–3212, New York, NY, USA. Association for Computing Machinery.	
978	Zafarani. 2020.		
979			
980			
981			
982			
983			
984	Xinyi Zhou and Reza Zafarani. 2019.	<a href="#">Network-based fake news detection: A pattern-driven approach</a> . <i>ArXiv</i> , abs/1906.04210.	
985			
986			
987	Xinyi Zhou and Reza Zafarani. 2020.	<a href="#">A survey of fake news: Fundamental theories, detection methods, and opportunities</a> . <i>ACM Comput. Surv.</i> , 53(5).	
988			
989			
990	Junyou Zhu, Chao Gao, Ze Yin, Xianghua Li, and Juer-	<a href="#">Propagation structure-aware graph transformer for robust and interpretable fake news</a> . In <i>Proceedings of the 30th ACM SIGKDD Conference on Knowledge Discovery and Data Mining</i> , KDD '24, page 4652–4663, New York, NY, USA. Association for Computing Machinery.	
991	gen Kurths. 2024.		
992			
			993
			994
			995
			996

## 997 A Methodology Details

998 **AGA.** In the AGA module, a learnable per-head  
999 temperature  $\tau_h$  is applied before softmax to normal-  
1000 ize the logits and produce attention weights  $\alpha_{i,j}^{(h)}$ :

$$1001 \alpha_{i,j}^{(h)} = \text{softmax}_j \left( \frac{\tilde{\mathbf{A}}_{i,j}^{(h)}}{\tau_h} \right) \quad (22)$$

1002 Each head output is then computed as a weighted  
1003 sum  $\mathbf{o}_i^{(h)}$  of values  $\mathbf{v}_j^{(h)}$ :

$$1004 \mathbf{o}_i^{(h)} = \sum_{j=1}^L \alpha_{i,j}^{(h)} \mathbf{v}_j^{(h)} \quad (23)$$

1005 and the final output of multi-head attention (MHA)  
1006 is:

$$1007 \text{MHA}(\mathbf{E}(x_i)) = \text{Concat}(\mathbf{o}_i^{(1)}, \dots, \mathbf{o}_i^{(H)}) \mathbf{W}_o \quad (24)$$

1008 where  $H$  is the number of attention heads in MHA  
1009 and  $\mathbf{W}_o$  is the weight matrix.

1010 **Entropy-gated Fusion.** Here, we formulate the  
1011 gate input vector  $\mathbf{u}$  as:

$$1012 \mathbf{u} = [\mathbf{h}; \mathbf{h}_E; \mathcal{H}(\hat{\mathbf{y}}_0); \mathcal{H}(\hat{\mathbf{y}}_E)] \quad (25)$$

1013 where  $\mathcal{H}(\hat{\mathbf{y}}_0)$ ,  $\mathcal{H}(\hat{\mathbf{y}}_E)$  are the entropy of Head<sub>0</sub> and  
1014 Head<sub>E</sub>.

1015 **Trainable Agreement Head.** In the trainable  
1016 agreement head scheme, we combine two streams  
1017 of features from both heads and add a new classifier  
1018 to learn how to jointly leverage them, instead of  
1019 directly fusing predictions. To construct agreement  
1020 features, we combine:

- 1021 • hidden states  $\mathbf{h}$  and  $\mathbf{h}_E$ ,
- 1022 • elementwise interaction ( $\mathbf{h} \odot \mathbf{h}_E$ ),
- 1023 • and absolute difference ( $|\mathbf{h} - \mathbf{h}_E|$ ).

1024 Formally, the agreement feature vector is defined  
1025 as:

$$1026 \phi_{\text{agree}} = [\mathbf{h}; \mathbf{h}_E; \mathbf{h} \odot \mathbf{h}_E; |\mathbf{h} - \mathbf{h}_E|]. \quad (26)$$

1027 Then, the agreement features are fed into the MLP  
1028 layers:

$$1029 \mathbf{z}_A = \mathbf{W}_2 \sigma(\mathbf{W}_1 \phi_{\text{agree}} + \mathbf{b}_1) + \mathbf{b}_2, \quad \mathbf{z}_A \in \mathbb{R}^K, \quad (27)$$

1030 where  $\mathbf{z}_A$  is agreement logits.  $\mathbf{W}_1$ ,  $\mathbf{W}_2$  and  $\mathbf{b}_1$ ,  $\mathbf{b}_2$   
1031 are learnable parameters. Finally, the agreement  
1032 head outputs predictions as:

$$1033 \mathbf{p}_A = \text{softmax}(\mathbf{z}_A). \quad (28)$$

1034 Here,  $\mathbf{p}_A$  is the "agreement head" prediction, which  
1035 learns to explore the consistency and discrepancy  
1036 between the two reasoning heads.

## 1037 B Experimental Model

1038 **Model Configuration.** Our detection pipeline em-  
1039 ploys a BiMind classifier, which effectively inte-  
1040 grates textual and knowledge features. Each in-  
1041 put token is represented by a 128-dimensional em-  
1042 bedding vector. The maximum sequence length  
1043 is 5000. In the transformer-based classifier mod-  
1044 ule, our model consists of 2 stacked transformer  
1045 encoder layers with a multi-head attention scheme  
1046 (i.e., 16 attention heads), producing pooled text  
1047 representations. We construct two heads: a content-  
1048 internal head that incorporates the text representa-  
1049 tions with the AGA module, and an external knowl-  
1050 edge head that injects the self-retrieval knowledge  
1051 vectors via FiLM before MLP. Here, we set  $k$  to 3  
1052 in the knowledge retrieval module. In the feature  
1053 fusion function, we set the entropy-gated strategy  
1054 as the default, where other options include a train-  
1055 able agreement head, standard logit average, and  
1056 product-of-experts. For the two heads, we employ  
1057 ReLU as an activation function and set dropout reg-  
1058 ularization to 0.3, where both heads are trained with  
1059 CE loss and a symmetric-KL agreement regular-  
1060 izer. To handle the class imbalance issue, we adopt  
1061 class-balanced weights on the CE loss. The final  
1062 output layer with a softmax function is designed  
1063 to provide the probability distribution indicating  
1064 the likelihood of the content being labeled 1 (i.e.,  
1065 correct information) or 0 (i.e., incorrect informa-  
1066 tion). Here, we use Adam optimizer with learning  
1067 rate  $1 \times 10^{-5}$  and batch size 64 to train our model,  
1068 where we employ the mixed-precision training, gra-  
1069 dient clipping, and early-stopping (patience = 3) to  
1070 tune the hyperparameters.

1071 **Experimental Models.** In our experimental  
1072 setup, we compared our BiMind model with five  
1073 tested models, including a CNN-based model (Kim,  
1074 2014), a GCN-based model (Yao et al., 2018), HAN  
1075 (Yang et al., 2016), BERT (Devlin et al., 2019),  
1076 and HeteroSGT (Zhang et al., 2024). More specifi-  
1077 cally, the CNN-based model employs CNN layers  
1078 to extract text features from article content and

then uses the extracted features to detect incorrect information. The GCN-based model explores the weighted graph built on news articles, which uses a GCN for identifying incorrect information. HAN applies word-level and sentence-level features in news content for incorrect information detection. Here, BERT is a transformer-based language model, similar to our transformer-based classifier, where we explore BERT to classify false content (i.e., incorrect information). HeteroSGT explores the heterogeneous subgraph transformer to classify articles via the heterogeneous graph.

Table 4: Statistics of the datasets used in our experiments.

Dataset	# Label 0	# Label 1	# Total	Avg. Length (words)
MM COVID	1,888	1,162	3,048	25
RoCOVery	605	1,294	1,899	500
LIAR	2,507	2,053	4,560	17
MC Fake	2,671	12,621	15,292	300

## C Dataset Statistics

Here, we present the statistics of the datasets we used, listed in Table 4.

**Dataset-level Knowledge Impact Analysis.** We conducted a comprehensive statistical analysis of knowledge impact across these datasets, as shown in Table 5. Based on these datasets, we observed substantial but different levels of vocabulary alignment between test instances and the knowledge bank (ranging from 75.60% to 81.68%), showing that retrieved knowledge is largely in-domain. But, retrieval relevance and its effects differ significantly. LIAR presents the lowest retrieval similarity (mean 0.6077), indicating weaker semantic alignment between its short claims and retrieved knowledge, which limits the efficiency of knowledge injection. In addition, MM COVID shows moderate similarity (mean 0.6870) with higher variance, revealing that knowledge retrieval is more sensitive and selective: for short and noisy social media posts, knowledge injection yields large positive VoX gains when relevant knowledge is retrieved.

In contrast, MC Fake and ReCOVery both exhibit consistently high retrieval similarity (means 0.7751 and 0.7567, respectively), suggesting that retrieval quality is not the primary bottleneck. Instead, linguistic complexity is the dominant factor: retrieved knowledge in these datasets presents extremely low Flesch Reading Ease scores, and knowledge impact varies primarily with how such

dense content is integrated rather than how relevant it is. In summary, these statistical results illustrate a spectrum of knowledge integration regimes, ranging from knowledge-limited (LIAR), to retrieval-sensitive (MM COVID), and finally to complexity-dominated settings (MC Fake, ReCOVery), motivating adaptive and uncertainty-aware mechanisms for mediating the impact of external knowledge.

## D Experimental Results

For the five comparison models, CNN has poor performance on all the datasets, which may result from its fixed convolutional kernels. Due to these kernels focusing on local features, the global features or dependencies might not be effectively explored in news articles and social contexts. GCN presents different results across multiple datasets and receives better detection accuracy on the MC Fake dataset. In addition, HAN and BERT are transformer-based models with attention mechanisms, and thus, the performance is comparable between them. Though HeteroSGT achieves optimal results, such as Rec and F1 on MC Fake due to its subgraph structure, it still drops performance by 19.1% on Acc and 19.1% on Pre, 5.2% on Acc and 5.7% on Pre, respectively, compared to our proposed model on ReCOVery and LIAR datasets. Typically, on the LIAR dataset, our model achieves consistent performance across seeds, with a low standard deviation ( $\pm 0.001$ ).

**Extended Experiments.** Here, we extended our dual-head design to other LLMs, i.e., RoBERTa (Liu et al., 2019) and DeBERTa (He et al., 2020). From Table 6, we can see that separating content-internal reasoning (Head<sub>0</sub>) from the knowledge-augmented reasoning (Head<sub>E</sub>) shows significant dataset-relevant behavior. On knowledge-aligned datasets, like ReCOVery and MM COVID, Head<sub>E</sub> consistently improves recall and F1 score, suggesting that external knowledge provides complementary contextual signals beyond textual content alone. In contrast, on the LIAR dataset with short claims and weak retrieval alignment, Head<sub>E</sub> is not generally helpful, supporting our motivation to disentangle content inference from knowledge-based reasoning rather than enforcing unconditional knowledge injection.

Additionally, the proposed uncertainty-aware fusion strategy achieves either the best or second-best performance across models and datasets. Notably, it reduces variance and receives gains when one

Table 5: Statistical comparison of knowledge attributes across datasets. Vocabulary alignment measures lexical intersection between inputs and the knowledge base. Retrieval relevance is reported as cosine similarity (mean  $\pm$  std). Flesch Reading Ease for the *helps* category reflects the linguistic complexity of retrieved knowledge.

Dataset	Vocab Alignment (%)	Max Sim.	Mean Sim.	Flesch ( <i>helps</i> )
LIAR	76.55	0.6603 $\pm$ 0.0924	0.6077 $\pm$ 0.0843	37.94
MM COVID	75.60	0.7586 $\pm$ 0.1228	0.6870 $\pm$ 0.1082	31.68
MC Fake	79.91	0.8176 $\pm$ 0.1084	0.7751 $\pm$ 0.1082	-280.47
ReCOVery	81.68	0.8056 $\pm$ 0.1071	0.7567 $\pm$ 0.1026	-585.00

head performs poorly, especially on LIAR dataset. These results validate our design choice to treat knowledge as an auxiliary, selectively trusted signal, with fusion strategy adapting to instance-level uncertainty rather than relying on static feature concatenation alone.

Together, the experimental results demonstrate that the effective and reliable knowledge injection (i) conditions on data-inherent attributes, including vocabulary alignment, retrieval relevance, and sample-level linguistic complexity, and (ii) requires a principled prediction fusion mechanism with uncertainty and agreement measurement.

## E Ablation Study

When removing the AGA, it leads to a significant drop in accuracy (0.897  $\rightarrow$  0.872) and F1 (0.895  $\rightarrow$  0.870), showing the importance of reshaping attention logits to prevent attention collapse. Without the knowledge retrieval function, it also reduces the performance, such as a larger drop in accuracy and recall (0.897  $\rightarrow$  0.847), indicating the significance of semantic knowledge neighbors in grounding short or ambiguous content. Additionally, replacing the uncertainty-aware fusions with a simple logit average, it causes performance degradation in F1 (0.895  $\rightarrow$  0.861 or 0.867), showing that our fusion strategies help the model adaptively trust knowledge-augmented predictions when content-internal predictions are uncertain. Finally, removing the symmetric KL regularizer, it reduces F1 from 0.895 to 0.874, demonstrating that agreement between heads stabilizes training and improves predictions.

In conclusion, ablation results show that each component contributes complementary benefits: content features construct strong baselines, attention geometries sharpen token-level salience, knowledge retrieval contextualizes content, and uncertainty fusion with an agreement regularizer ensures robust integration. In an explicit and structured way, these modules jointly enable BiMind

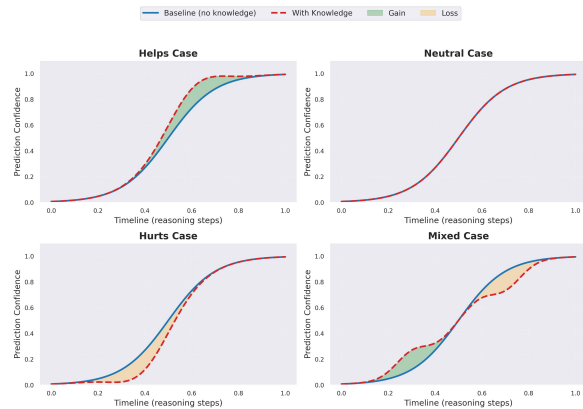


Figure 4: An illustration of knowledge impacts at the instance level. Blue curve = baseline (no knowledge), red dashed curve = with knowledge, shaded regions indicate gain (green) or loss (orange).

to achieve both competitive performance and interpretable diagnostics on when and why knowledge matters.

## F VoX Analysis

To further interpret the VoX values, we visualized four types of knowledge impacts in Figure 4, which demonstrates how knowledge can impact prediction confidence over the reasoning path. Typically, knowledge can help (e.g., MM COVID), be neutral, hurt (e.g., LIAR), or produce mixed patterns (e.g., MC Fake) from the dataset-level outcomes.

## G Quantitative Analysis

Here, we describe the running time comparison of our BiMind framework with backbone Sentence-Transformer and HeteroSGT in the application of incorrect information detection.

Beyond superior detection accuracy, we compared the runtime of BiMind against HeteroSGT on all the benchmark datasets shown in Table 7. In our framework, we skip the graph construction phase, resulting in training and testing that is nearly 4 $\times$  faster (e.g., on the dataset MM COVID). HeteroSGT requires additional graph construction time

Table 6: Extended performance comparison (mean  $\pm$  std, in %, across 10 runs, best in **bold**).

Model	Dataset	Head/Mode	Acc	F1	Pre	Rec
LLaMA-7B	ReCOVery	Head <sub>0</sub>	91.13 $\pm$ 2.34	91.03 $\pm$ 2.59	91.35 $\pm$ 2.32	91.13 $\pm$ 2.34
		Head <sub>E</sub>	91.04 $\pm$ 1.18	91.09 $\pm$ 1.21	91.53 $\pm$ 1.44	91.04 $\pm$ 1.18
		Fused	<b>91.82 <math>\pm</math> 1.29</b>	<b>91.86 <math>\pm</math> 1.27</b>	<b>92.20 <math>\pm</math> 1.26</b>	<b>91.82 <math>\pm</math> 1.29</b>
	MM COVID	Head <sub>0</sub>	94.69 $\pm$ 1.01	94.70 $\pm$ 1.01	94.46 $\pm$ 1.45	94.67 $\pm$ 0.99
		Head <sub>E</sub>	94.80 $\pm$ 0.77	94.81 $\pm$ 0.76	94.48 $\pm$ 1.21	94.61 $\pm$ 0.64
		Fused	<b>95.12 <math>\pm</math> 0.78</b>	<b>95.12 <math>\pm</math> 0.78</b>	<b>94.98 <math>\pm</math> 1.06</b>	<b>95.08 <math>\pm</math> 0.86</b>
	LIAR	Head <sub>0</sub>	<b>63.26 <math>\pm</math> 0.13</b>	<b>63.26 <math>\pm</math> 0.19</b>	63.70 $\pm$ 0.20	63.60 $\pm$ 0.30
		Head <sub>E</sub>	62.70 $\pm$ 0.41	62.42 $\pm$ 0.53	<b>64.00 <math>\pm</math> 0.20</b>	63.60 $\pm$ 0.30
		Fused	62.93 $\pm$ 0.29	62.89 $\pm$ 0.29	63.80 $\pm$ 0.20	<b>63.70 <math>\pm</math> 0.20</b>
DeBERTa-v3	ReCOVery	Head <sub>0</sub>	81.38 $\pm$ 2.95	81.64 $\pm$ 2.71	83.85 $\pm$ 1.80	81.38 $\pm$ 2.70
		Head <sub>E</sub>	85.72 $\pm$ 1.43	85.92 $\pm$ 1.25	86.39 $\pm$ 1.30	85.32 $\pm$ 1.30
		Fused	<b>85.81 <math>\pm</math> 1.27</b>	<b>85.94 <math>\pm</math> 1.16</b>	<b>86.42 <math>\pm</math> 1.20</b>	<b>85.81 <math>\pm</math> 0.90</b>
	MM COVID	Head <sub>0</sub>	93.00 $\pm$ 1.23	92.98 $\pm$ 1.24	93.07 $\pm$ 1.20	92.73 $\pm$ 1.40
		Head <sub>E</sub>	<b>94.59 <math>\pm</math> 1.05</b>	<b>94.59 <math>\pm</math> 1.05</b>	<b>94.47 <math>\pm</math> 1.20</b>	<b>94.56 <math>\pm</math> 1.00</b>
		Fused	94.53 $\pm$ 1.09	94.54 $\pm$ 1.08	94.43 $\pm$ 1.30	94.47 $\pm$ 1.10
	LIAR	Head <sub>0</sub>	59.75 $\pm$ 0.89	59.14 $\pm$ 1.21	61.70 $\pm$ 0.50	60.80 $\pm$ 0.50
		Head <sub>E</sub>	<b>62.05 <math>\pm</math> 0.77</b>	<b>62.02 <math>\pm</math> 0.94</b>	<b>62.50 <math>\pm</math> 0.50</b>	<b>62.50 <math>\pm</math> 0.60</b>
		Fused	61.91 $\pm$ 0.78	61.87 $\pm$ 1.00	62.50 $\pm$ 0.50	62.40 $\pm$ 0.60
RoBERTa	ReCOVery	Head <sub>0</sub>	81.28 $\pm$ 2.96	81.67 $\pm$ 2.60	80.36 $\pm$ 2.20	82.84 $\pm$ 1.74
		Head <sub>E</sub>	84.53 $\pm$ 2.10	84.71 $\pm$ 2.19	83.97 $\pm$ 1.16	85.76 $\pm$ 0.74
		Fused	<b>84.93 <math>\pm</math> 2.45</b>	<b>85.12 <math>\pm</math> 2.54</b>	<b>83.92 <math>\pm</math> 1.76</b>	<b>86.13 <math>\pm</math> 1.06</b>
	MM COVID	Head <sub>0</sub>	91.87 $\pm$ 1.23	91.88 $\pm$ 1.23	92.25 $\pm$ 1.44	91.87 $\pm$ 1.23
		Head <sub>E</sub>	<b>94.49 <math>\pm</math> 0.26</b>	<b>94.49 <math>\pm</math> 0.27</b>	<b>94.59 <math>\pm</math> 0.26</b>	<b>94.49 <math>\pm</math> 0.26</b>
		Fused	94.21 $\pm$ 0.44	94.22 $\pm$ 0.44	94.40 $\pm$ 0.55	94.21 $\pm$ 0.44
	LIAR	Head <sub>0</sub>	61.18 $\pm$ 0.77	60.83 $\pm$ 0.83	62.37 $\pm$ 0.17	61.91 $\pm$ 0.25
		Head <sub>E</sub>	<b>61.88 <math>\pm</math> 0.63</b>	<b>61.84 <math>\pm</math> 0.73</b>	<b>62.71 <math>\pm</math> 0.25</b>	<b>62.55 <math>\pm</math> 0.34</b>
		Fused	61.83 $\pm$ 0.66	61.68 $\pm$ 0.78	62.67 $\pm$ 0.29	62.47 $\pm$ 0.41

Table 7: Performance and runtime comparison between **BiMind** and **HeteroSGT** across four benchmark datasets. Performance is reported as mean  $\pm$  std. Runtime is measured in seconds per run.

Dataset	Model	Acc	Pre	Rec	F1	Training	Testing	Graph
MM COVID	HeteroSGT	0.915 $\pm$ 0.009	0.905 $\pm$ 0.011	0.883 $\pm$ 0.013	0.893 $\pm$ 0.011	55.11	–	13.62
	BiMind	<b>0.902<math>\pm</math>0.116</b>	<b>0.902<math>\pm</math>0.110</b>	<b>0.898<math>\pm</math>0.142</b>	<b>0.900<math>\pm</math>0.132</b>	15.19	0.08	–
ReCOVery	HeteroSGT	0.727 $\pm$ 0.023	0.731 $\pm$ 0.047	0.585 $\pm$ 0.036	0.571 $\pm$ 0.049	21.94	–	9.03
	BiMind	<b>0.879<math>\pm</math>0.017</b>	<b>0.862<math>\pm</math>0.028</b>	<b>0.843<math>\pm</math>0.203</b>	<b>0.854<math>\pm</math>0.208</b>	14.99	0.10	–
MC Fake	HeteroSGT	0.883 $\pm$ 0.002	0.812 $\pm$ 0.003	0.762 $\pm$ 0.002	0.783 $\pm$ 0.003	478.53	–	40.04
	BiMind	<b>0.887<math>\pm</math>0.051</b>	<b>0.827<math>\pm</math>0.016</b>	<b>0.700<math>\pm</math>0.099</b>	<b>0.798<math>\pm</math>0.109</b>	153.01	0.45	–
LIAR	HeteroSGT	0.581 $\pm$ 0.002	0.580 $\pm$ 0.003	0.575 $\pm$ 0.002	0.571 $\pm$ 0.003	116.22	–	14.48
	BiMind	<b>0.605<math>\pm</math>0.041</b>	<b>0.601<math>\pm</math>0.045</b>	<b>0.595<math>\pm</math>0.037</b>	<b>0.595<math>\pm</math>0.037</b>	73.51	0.52	–

(e.g., 40.04s on MC Fake) and retraining to adapt to new topics; however, BiMind generalizes with lightweight attention signals and in-memory knowledge features. It shows BiMind’s efficiency and

scalability merits in real-world applications.

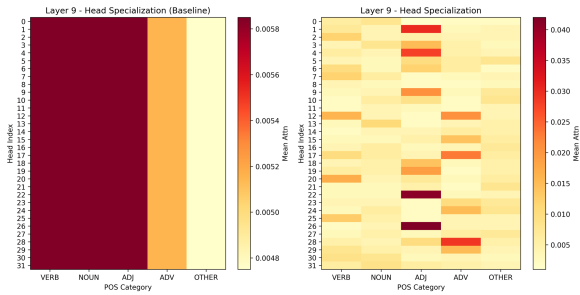


Figure 5: Layer 9 attention head specialization with and without AGA. Left: Baseline Transformer without AGA. Right: Transformer with AGA.

## H Attention Head Specialization

Figure 5 compares attention head specialization at Layer 9 of the Transformer with and without AGA. For the baseline model, the attention heads present severe representational collapse: all heads have nearly identical attention patterns, with uniformly high focus on several categories (VERB, NOUN, ADJ) and minimal head-level variance. It shows that, without AGA, self-attention mechanism tends to flatten linguistic structure in deeper layers. However, with AGA, it shows a significantly different geometric behavior. The number of active heads is reduced, but the head specialization is selectively preserved where a small number of heads focus on different categories (like ADJ and ADV). Specially, head specialization remains diverse rather than uniform. It demonstrates that AGA transforms attention collapse into geometry-aware concentration, compressing distributed signals into a low-rank but structured representation.

## I Data Access

Our BiMind model and all the tested datasets in our work are accessible via the link: <https://file.fast/59b1W/supplementary-materials.zip>